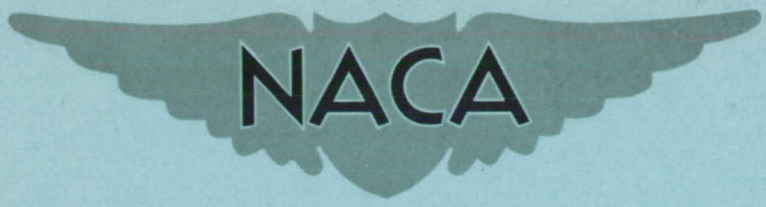

RESEARCH MEMORANDUM

EFFECT OF CIRCUMFERENTIAL TOTAL-PRESSURE GRADIENTS TYPICAL OF SINGLE-INLET DUCT INSTALLATIONS ON PERFORMANCE OF AN AXIAL-FLOW TURBOJET ENGINE

By S. C. Huntley, Joseph N. Sivo, and
Curtis L. Walker

Lewis Flight Propulsion Laboratory
Cleveland, Ohio

NATIONAL ADVISORY COMMITTEE
FOR AERONAUTICS

WASHINGTON

June 3, 1955
Declassified September 29, 1960

NATIONAL ADVISORY COMMITTEE FOR AERONAUTICS

RESEARCH MEMORANDUM

EFFECT OF CIRCUMFERENTIAL TOTAL-PRESSURE GRADIENTS TYPICAL OF SINGLE-INLET DUCT INSTALLATIONS ON PERFORMANCE OF AN AXIAL-FLOW TURBOJET ENGINE

By S. C. Huntley, Joseph N. Sivo, and Curtis L. Walker

SUMMARY

An investigation was conducted in an NACA Lewis altitude test chamber to determine the effect of circumferential total-pressure gradients at the compressor inlet, typical of those resulting from a single inlet duct, on the component and over-all performance of an axial-flow turbojet engine. Two magnitudes of total-pressure gradient, 15 and 20 percent at rated corrected engine speed, were investigated in addition to a uniform distribution. At Reynolds number indices of 0.6 and 0.2, data were obtained at corrected engine speeds from 60 to 105 percent of rated speed over a range of exhaust-gas temperatures at each speed.

The circumferential pressure gradients persisted through the compressor but decreased in severity. However, the turbine temperature gradient caused by the inlet-pressure gradient necessitated a reduction in average turbine-inlet temperature to avoid local overtemperaturing which could result in turbine failure. As a result, the net thrust was reduced 9 and 14 percent at altitudes of 22,000 and 50,000 feet, respectively, for a flight Mach number of 0.6. In addition, a 14 percent net thrust loss resulted from the reduction in average inlet total pressure due to the pressure gradient. Associated with these total net thrust losses are increases in specific fuel consumption of 6 and 9 percent for altitudes of 22,000 and 50,000 feet, respectively.

INTRODUCTION

In aircraft installations of turbojet engines, both radial and circumferential variations of total pressure at the compressor inlet are usually present. These pressure variations are due to asymmetric or separated air flow resulting from curved ducts, high angles of attack, or yaw. Circumferential variations in inlet total pressure, as shown in references 1 and 2, affected flow conditions through the entire

engine and resulted in losses in compressor efficiency, air flow, and thrust with increased specific fuel consumption. Compressor stall or surge or even engine destruction can also result from inlet-air distortion (ref. 2).

In references 1 and 2, compressor-inlet conditions similar to those which might be encountered in flight with twin-inlet ducts were simulated. For the reference tests, an abrupt discontinuity of air flow was imposed at the compressor inlet by a uniform blockage of one inlet duct with fine mesh screens. A single inlet duct, however, imposes more gradual pressure gradients at the compressor inlet than a twin inlet. Therefore, as part of an extensive program to evaluate the effects of inlet-air distortion, an investigation was conducted in an altitude test chamber at the NACA Lewis laboratory to determine the effect of circumferential total-pressure gradients typical of single inlet ducts on the performance of the axial-flow turbojet engine of reference 2. The results of this investigation are reported herein.

Two circumferential total-pressure gradients that might be encountered in flight with a single-inlet duct were simulated. Unpublished data from wind-tunnel tests of single-inlet ducts indicated that the circumferential gradients usually encountered were approximately sinusoidal with one low-pressure region. Two such gradients were approximated by blocking the compressor inlet with graduated screen densities around the circumference. The magnitudes of the gradients investigated were 15 and 20 percent of the average inlet total pressure at rated corrected engine speed.

Data were obtained from 60 to 105 percent of rated corrected engine speed over a range of exhaust-gas temperatures at each speed and at Reynolds number indices of 0.6 and 0.2. These Reynolds number indices are equivalent to inlet conditions corresponding to a range of flight conditions; for example, at a flight Mach number of 0.6, a Reynolds number index of 0.6 corresponds to an altitude of 22,000 feet and an index of 0.2 to an altitude of 50,000 feet. The effect of inlet-pressure distortion on net thrust and specific fuel consumption at these two flight conditions is discussed. Pressure and temperature profiles, component, and over-all engine performance are also discussed. A comparison is also made with the results of distortions with twin-inlet ducts (ref. 2) on the same engine.

APPARATUS AND PROCEDURE

Engine and Installation

A schematic sketch of the turbojet engine as it was installed in one of the NACA Lewis altitude test chambers is shown in figure 1. This

engine had a 12-stage axial-flow compressor, eight can-type combustors, and a single-stage turbine. The sea-level static thrust rating is 5970 pounds at an engine speed of 7950 rpm and an exhaust-gas temperature of 1275° F. Exhaust-nozzle flaps were used to obtain a range of exhaust-gas temperatures at each engine speed.

A 1/4-inch mesh screen was placed over the entire annulus approximately 37 inches upstream of the inlet guide vanes. Segments of fine screen were then supported on this 1/4-inch mesh to obtain the desired distortion. Sketches of the inlet-screen configurations used are shown in figure 2.

Instrumentation

Instrumentation for measuring temperatures and pressures was installed at stations indicated in figure 1. Details of the instrument stations are shown in figure 3. In addition, four nozzle-lip static probes were used to determine the exhaust-nozzle-discharge static pressure.

A magnetic pickup, described in reference 2, was installed in the compressor to detect vibration of the first-stage rotor blades. This pickup was installed in the first stage primarily because that was the only location feasible from mechanical considerations.

Constant-temperature hot-wire anemometers were used for detection of flow fluctuations caused by rotating stall. The anemometer probes used 0.0002-inch-diameter tungsten wire with an unplated length (effective length) of 0.08 inch. The wire element was mounted perpendicular to the probe axis. Four anemometer probes, located at 90° circumferential intervals, were installed in radial-survey devices in the compressor fourth-stage stator.

Procedure

Data were obtained at the conditions described in table I. Reynolds number index was maintained constant at station 1. Average values of temperature, pressure, and engine speed for each condition are given.

Several data points were obtained at each value of engine speed over a range of exhaust-gas temperatures by varying the exhaust-nozzle area. An indicated local turbine-inlet temperature of 2260° R was used as the operating limit. Operation was arbitrarily limited to this local value of turbine-inlet temperature after failure of a turbine attributed to excessive local temperature (ref. 2).

For all the performance data presented herein the average pressures and temperatures at each station were obtained by area-weighting all the individual values. These average values of pressures and temperatures, which represent flow conditions for an incompressible fluid, closely approximated the more exact values obtained by satisfying one-dimensional considerations of continuity, momentum, and energy for the magnitude of pressure gradients investigated. This second method, while more exact, requires a laborious solution to obtain the effective values of pressure and temperature. Therefore, the effective values were used only to make a comparison of compressor performance at one engine operating condition between a uniform inlet pressure gradient, an abrupt circumferential gradient (ref. 2), and the sinusoidal gradient that is reported herein. Symbols used in this report are defined in appendix A and the methods of calculation are described in appendix B.

RESULTS AND DISCUSSION

Pressure and Temperature Profiles

The effect of inlet-air distortion on compressor circumferential total-pressure and -temperature profiles is shown in figure 4. These data are for operation at rated corrected engine speed and at a Reynolds number index of 0.6. The ordinate for each profile was obtained by first dividing the individual probe values by the average value to put all profiles on a comparative basis, and, second, dividing this ratio by that for the undistorted condition (configuration A) to eliminate small circumferential variations in the undistorted profiles. The abscissa is the circumferential location of individual probes measured counterclockwise from the top (in the direction of rotor rotation) while looking downstream. Each profile shape is nearly sinusoidal and is typical of all conditions investigated for each configuration. It is shown (fig. 4) that the magnitude of the total-pressure gradient decreased, while passing through the compressor, from 15 to about 2 percent for configuration B and from 20 to 4 percent for configuration C. Although the percentage pressure difference decreased, the absolute pressure difference was essentially maintained through the compressor. A similar trend was found for the investigation of reference 2. The circumferential locations of the least and greatest blockage are indicated in figure 4(a). A comparison of the profiles of figures 4(a) and (b) indicates that the high- and low-pressure regions rotated about 60° in the direction of rotor rotation while passing through the compressor.

Compressor-outlet total temperature in the low-pressure region is higher than in the high-pressure region (fig. 4(c)) because of the higher compressor pressure ratio across the low inlet-pressure segment.

Turbine-inlet circumferential total-temperature profiles were not recorded. (The instrumentation at that station was used only as an indication of excessive local temperature.) Turbine-outlet total-temperature profiles based on individual rake averages are shown in figure 5 for the same conditions as the data in figure 4. The magnitude of total-temperature variation at the turbine outlet was greater than that at the compressor outlet. This greater magnitude of turbine-outlet-temperature variation results mainly from a circumferential variation in fuel-air ratio caused by the distorted air flow. The limited measurements were inadequate to explain the change in profile shape from that at the compressor outlet. No radial-temperature-profile shift was discernible.

The effect of corrected engine speed and Reynolds number index on the amplitude of compressor-inlet total-pressure gradient is presented in figure 6 which also illustrates the magnitude of the distortions used. As engine speed was increased, the higher air velocity across the screens and attendant greater pressure loss resulted in an increase in amplitude; Reynolds number index had a negligible effect on the amplitude. At rated corrected engine speed, configuration B resulted in a compressor-inlet total-pressure variation of 15 percent and with configuration C of 20 percent.

Component Performance

The effect of air distortion from twin-inlet ducts on component performance that was established on this engine in reference 2 showed that the distortions had a negligible effect on combustor and turbine performance. Also, at any given engine speed, each circumferential half of the compressor essentially shifted its respective performance point along a constant speed line on the compressor map. The inlet distortions reported herein were less severe in peak magnitude of pressure variation and also showed a negligible effect on combustor and turbine performance.

The effect of the inlet-air distortions of the present investigation on compressor performance is presented in figures 7 to 9. Over-all values of corrected compressor air flow, pressure ratio, and efficiency are shown. Each parameter is based on average values of total pressure or temperature at either the compressor inlet (station 2) or outlet (station 3) as discussed in the Procedure. At a given corrected engine speed, corrected air flow decreased slightly with an increase in distortion for the range of conditions investigated (fig. 7). The decrease in air flow was negligible at high corrected engine speeds and at a Reynolds number index of 0.6. At a Reynolds number index of 0.2, the decrease in air flow was more pronounced. Compressor efficiency also decreased with an increase in distortion and this decrease was slightly more pronounced at the lower value of Reynolds number index (fig. 8).

The effect of the inlet distortions of this investigation on compressor pressure ratio as a function of engine total-temperature ratio is shown in figure 9. From these curves an engine operating point on the compressor map may be determined. For a constant value of engine total-temperature ratio, compressor pressure ratio by continuity of flow is primarily a function of corrected compressor air flow and turbine total-temperature ratio when critical flow exists in the turbine nozzle. Turbine total-temperature ratio, in turn, is directly related through power requirements to compressor pressure ratio and compressor efficiency. Consequently, the change in compressor pressure ratio for constant-corrected-engine-speed and constant-engine-total-temperature-ratio operation is primarily a result of the effect of distortion on corrected compressor air flow and efficiency. For constant corrected engine speed and constant engine total-temperature ratio, the change in compressor pressure ratio with inlet-air distortion was negligible at a Reynolds number index of 0.6 (fig. 9(a)). At the lower value of Reynolds number index, 0.2, and at high values of corrected engine speed, compressor pressure ratio decreased with distortion at a constant engine total-temperature ratio (fig. 9(b)).

A comparison between the over-all compressor performance for a sinusoidal, an abrupt discontinuity, and an undistorted circumferential pressure variation at the compressor inlet is shown in the following table for engine operation at rated corrected engine speed, a corrected exhaust-gas temperature of 1800° R, and a Reynolds number index of 0.6:

Type of distortion	Percent magnitude of inlet total-pressure variation	Corrected compressor air flow, $\frac{W_{a,2}\sqrt{\theta_2}}{\delta_2}$	Compressor pressure ratio, $\frac{P_3}{P_2}$	Compressor efficiency, η_c
Undistorted	0	107.5	5.50	0.78
Sinusoidal	20	107.1	5.52	.78
Abrupt discontinuity	32	105.4	5.46	.80

Data for the abrupt discontinuity-type distortion were obtained from reference 2. These data from reference 2 and the data from the present investigation were put on a common basis for comparison by using effective values of total pressure and total temperature that represented one-dimensional flow at both the compressor inlet and outlet. The method used to obtain these effective values and the necessary assumptions are discussed in the procedure and in appendix B. The magnitude of inlet-pressure variation was different for each distortion (see preceding table); these magnitudes were selected for this comparison because they correspond to the maximum variation obtained from wind-tunnel tests of typical inlet ducts.

A comparison of the values given in the preceding table shows that either type of distortion had only a slight effect on over-all compressor performance. The data used for this comparison were obtained at a Reynolds number index of 0.6 and for engine operation at rated corrected engine speed with a corrected exhaust-gas temperature of 1800° R. Although the over-all compressor performance was not affected a great deal at the engine operating condition selected for this comparison, the compressor operable speed range will be reduced as the magnitude of distortion is increased because of compressor stall (see ref. 2). No steady-state compressor stall or surge was encountered during the present investigation.

Instrumentation was installed during the present investigation to detect rotating stall and first-stage rotor-blade vibrations. No rotating stall or high first-stage rotor-blade vibratory stresses were encountered in the compressor.

Engine Pumping Characteristics

Engine pumping characteristics were used to calculate over-all engine performance for particular flight conditions. (The method of calculation is presented in appendix B.) The effect of inlet-air distortion on engine pumping characteristics is presented in figure 10. Each parameter was based on average values of pressure and temperature as previously mentioned. The data were limited by a local turbine-inlet-temperature limit of 2260° R. Cross marks on some of the curves indicate the engine total-pressure ratio required to choke the exhaust nozzle; data below this point served only to help establish the trend of the generalized data because the "unchoked" data have only a limited application to other flight conditions.

At constant corrected engine speed and constant engine total-temperature ratio, an increase in distortion resulted in a decrease in engine total-pressure ratio. This decrease in engine total-pressure ratio was more pronounced at the lower Reynolds number index (0.2) and at intermediate corrected engine speeds and reflects the change in compressor performance with distortion.

Net Thrust and Net Thrust Specific Fuel Consumption

Net thrust with no distortion was calculated assuming no inlet-duct loss and with an average exhaust-gas total temperature of 1760° R. Engine speed and exhaust-nozzle area were then adjusted to give maximum net thrust. With distortion, maximum net thrust was determined in a similar manner except that the average exhaust-gas temperature was reduced so as not to exceed a local turbine-inlet temperature of 2260° R.

In addition, an inlet-duct loss in average total pressure sufficient to cause the distortion was assumed; that is, maximum local total pressure at the compressor inlet was considered to be that corresponding to free-stream total pressure.

Maximum net thrust determined in the manner just described is shown in figure 11 for operation at a flight Mach number of 0.6 and an altitude of 22,000 feet. Maximum net thrust decreased 24 percent with the most severe distortion of this investigation and net thrust specific fuel consumption increased 6 percent. Several factors are involved in this thrust decrease, namely: (1) loss in compressor performance, (2) decrease in average exhaust-gas temperature and, (3) reduction in average compressor-inlet total pressure. The losses in maximum net thrust incurred by each of these factors were successively determined and are also shown in figure 11. With the assumption of no inlet-duct loss and with an average exhaust-gas temperature of 1760° R, the net thrust decreased about 1 percent with the most severe distortion because of the effect of pressure gradients on compressor performance. Because of the circumferential temperature profile existing at the turbine, it was necessary to decrease the average exhaust-gas temperature 135° F with the most severe distortion to avoid exceeding a limiting local turbine-inlet temperature. This reduction in average exhaust-gas temperature resulted in an additional 9 percent loss in net thrust. The remaining thrust loss of 14 percent results from the decrease in average inlet total pressure caused by the pressure gradient. The maximum-net-thrust mode of engine operation selected for this discussion required a slight increase in effective exhaust-nozzle area. A further decrease in thrust would result for any other mode of operation.

Maximum net thrust as a function of percentage distortion at a flight Mach number of 0.6 and an altitude of 50,000 feet is shown by the curve of figure 12. A 29-percent loss in maximum net thrust was incurred with the most severe distortion of this investigation, and net thrust specific fuel consumption increased 9 percent. This loss in thrust occurred with an 18.8-percent variation in engine-inlet total pressure and at a corrected engine speed of 95 percent of rated. Average exhaust-gas temperature was 160° F lower with this distortion than for the undistorted engine and there was a slight increase in exhaust-nozzle area.

If engine operation with distortion were based on an average exhaust-gas temperature limit rather than a local turbine-inlet temperature limit, it would have been necessary to derate the undistorted engine to prevent excess local temperatures that occur with distortion. Maximum net thrust for such engine operation is shown in figure 12 by the solid data points. The average exhaust-gas temperature limit was selected as that required for operation with the most severe distortion of this investigation (configuration C). With no distortion there was a

13-percent loss in maximum net thrust. Net thrust specific fuel consumption also decreased with the derated operation in the undistorted engine as a result of higher component efficiencies at lower engine speed. A similar derating of thrust was required for safe operation with the inlet-air distortion used in reference 2.

CONCLUDING REMARKS

An investigation was conducted to determine the effect of circumferential total-pressure gradients at the compressor inlet on the performance of an axial-flow turbojet engine. The circumferential pressure gradients persisted through the compressor but decreased in severity. A slight temperature gradient existed with the pressure gradient at the compressor outlet which increased in magnitude at the combustor outlet. For the magnitude of the pressure gradients investigated the performance of the engine components was relatively unaffected. However, the temperature gradient existing at the turbine necessitated a reduction in average turbine-inlet temperature to avoid local overtemperaturing which could result in turbine failure. As a result, the pressure gradient effect on the internal characteristics of the engine reduced the net thrust 10 and 15 percent at altitudes of 22,000 and 50,000 feet, respectively, for a flight Mach number of 0.6. An additional loss in thrust of 14 percent occurred because of the decrease in average inlet total pressure caused by the pressure gradient. Associated with these total net thrust losses are increases in specific fuel consumption of 6 and 9 percent for altitudes of 22,000 and 50,000 feet, respectively.

Lewis Flight Propulsion Laboratory
National Advisory Committee for Aeronautics
Cleveland, Ohio, December 15, 1954

APPENDIX A

SYMBOLS

The following symbols are used in this report:

A	area, sq ft
F_n	net thrust, lb
f	fuel-air ratio
g	acceleration due to gravity, ft/sec^2
N	engine speed, rpm
P	total pressure, lb/sq ft
p	static pressure, lb/sq ft
T	total temperature, $^{\circ}R$
V	velocity, ft/sec
W_a	air flow, lb/sec
W_f	fuel flow, lb/hr
γ	ratio of specific heats
δ	ratio of compressor-inlet total pressure P_2 to NACA standard sea-level pressure, $P_2/2116$
θ	ratio of engine-inlet total temperature T_1 to NACA standard sea-level temperature, $T_1/519$
η	efficiency
φ	ratio of coefficient of viscosity corresponding to T_1 to coefficient of viscosity corresponding to NACA standard sea-level temperature. This ratio is a function of temperature only and is equal to $7350\theta^{1.5}/(T_1 + 216)$.
$\frac{\delta}{\varphi\sqrt{\theta}}$	Reynolds number index

Subscripts:

ave	average
CL	compressor leakage air flow
c	compressor
i	indicated
j	vena contracta at exhaust nozzle outlet
max	maximum
min	minimum
0	ambient or free-stream conditions
1	engine inlet
2	compressor inlet
3	compressor outlet or combustor inlet
4	combustor outlet or turbine inlet
5	turbine outlet
9	exhaust-nozzle inlet

APPENDIX B

METHODS OF CALCULATION

Average Values of Total Pressure and Total Temperature

The compressor-inlet total-pressure, compressor-outlet total-pressure, and compressor-outlet total-temperature gradients were nearly sinusoidal. An arithmetic average of two radial measurements at diametrically opposite locations resulted, therefore, in area-weighted values at these stations. For the range of conditions investigated the average values obtained in this manner closely approximated effective values obtained by a more exact procedure and were deemed adequate for the presentation of performance data.

Effective Values of Total Pressure and Total Temperature

Effective values of total pressure and total temperature at the compressor inlet and outlet were calculated for engine operation at a Reynolds number index of 0.6, rated corrected engine speed, and a corrected exhaust-gas temperature of 1800° R. These effective values were used to obtain a common basis for comparison of the data from a sinusoidal, an abrupt discontinuity, and an undistorted circumferential pressure variation at the compressor inlet. In order for the comparison to be accurate, the effective values of pressure and temperature must be true representations of the flow properties of the air which simultaneously satisfies the total energy, mass flow, and total momentum of the real flow. The total quantities of energy, mass flow, and momentum were obtained at the compressor inlet and outlet by integration. In order to perform the integration the following assumptions were made: For the sinusoidal distortion the compressor-inlet axial Mach number and the compressor-outlet static pressure were assumed constant. With an abrupt discontinuity distortion, compressor-outlet static pressure was assumed constant and continuity was maintained through each portion of the compressor subjected to the high and low inlet pressures. Also, as discussed in reference 2, the air flow through the high-inlet-pressure portion was the same as that for the undistorted case. The total quantities of energy, mass flow, and momentum were equated to one-dimensional equations expressed in terms of pressure, temperature, and Mach number. A simultaneous solution of these three equations resulted in one set of values of pressure, temperature, and Mach number which were designated as effective values representing one-dimensional flow. These effective values representing one-dimensional flow agree exactly with the values of pressure and temperature determined by area weighting for the undistorted pressure variation at the compressor inlet. As the severity of the distortion is increased, area weighting the individual pressures and

temperatures becomes a less accurate representation of the over-all effective values of pressures and temperatures because the area-weighting procedure essentially assumes incompressible flow.

Engine Air Flow

The air flow was determined at station 2 using the continuity equation with average total and static pressures and an effective area for this station, and the total temperature at station 1. The average pressures used were arithmetic averages of radial measurements behind the least and greatest blockage. The effective area was calibrated during the investigation of configuration A (1/4-in. screen only).

Compressor Efficiency

The efficiency was calculated from the conventional adiabatic equation assuming a constant specific heat. All pressures and temperatures used were area-weighted average values of two radial measurements at diametrically opposite locations.

Net Thrust

In determining the net thrust, the following items were assumed: (1) altitude (NACA standard atmosphere); (2) flight Mach number; (3) ram-pressure recovery; (4) exhaust-gas temperature; and (5) corrected engine speed.

The first three items define p_0, V_0, P_2, T_1, δ, and θ. Compressor-inlet total temperature T_1 and item (4) determine engine total-temperature ratio T_9/T_1. From engine pumping characteristics (fig. 11) and T_9/T_1, the engine total-pressure ratio P_9/P_2 was determined. Compressor pressure ratio P_3/P_2 was determined from figure 9. From P_3/P_2, $N/\sqrt{\theta}$ and figure 7, the corrected air flow $\frac{W_{a,2}\sqrt{\theta_2}}{\delta_2}$ was determined. The thrust equation was

$$F_n = \left[(1 + f)(W_{a,2} - W_{CL})V_j + A_j(p_j - p_0)\right] - \frac{W_{a,2}V_0}{g}$$

The part of this equation enclosed by brackets can be solved by use of the effective velocity parameter of reference 3, $(W_{a,2} - W_{CL})$, T_9, γ_9, and p_0/P_9. The compressor leakage flow W_{CL} was determined from P_3 and figure 13. Engine fuel-air ratio f was determined using T_9/T_1, θ, and figure 14.

Net Thrust Specific Fuel Consumption

The net thrust specific fuel consumption was determined from the following equation:

$$sfc = \frac{W_f}{F_n}$$

REFERENCES

1. Wallner, Lewis E., Conrad, E. William, and Prince, William R.: Effect of Uneven Air-Flow Distribution to the Twin Inlets of an Axial-Flow Turbojet Engine. NACA RM E52K06, 1953.

2. Walker, Curtis L., Sivo, Joseph N., and Jansen, Emmert T.: Effect of Unequal Air-Flow Distribution from Twin Inlet Ducts on Performance of an Axial-Flow Turbojet Engine. NACA RM E54E13, 1954.

3. Turner, L. Richard, Addie, Albert N., and Zimmerman, Richard H.: Charts for the Analysis of One-Dimensional Steady Compressible Flow. NACA TN 1419, 1948.

TABLE I. - CONDITIONS AT WHICH PERFORMANCE DATA WERE OBTAINED

Reynolds number index, $\frac{\delta_1}{\Phi_1\sqrt{\theta_1}}$	Corrected engine speed, $N/\sqrt{\theta_1}$, percent of rated	Engine-inlet total temperature, T_1, $^{\circ}R$	Compressor-inlet total pressure, P_2, lb/sq ft	Engine speed, rpm
Configuration A (undistorted)				
0.6	60	533	1302	4824
	80	458	1040	5960
	88	457	1026	6544
	95	458	1007	7068
	100	459	1011	7465
	105	410	868	7546
0.2	80	534	430	6447
	88	412	302	6224
	95	413	301	6745
	100	422	302	7160
	105	416	288	7570
Configuration B (15 percent)				
0.6	95	459	936	7115
	100	460	924	7483
	105	418	805	7520
0.2	95	429	289	6839
	100	430	289	7185
	105	431	281	7502
Configuration C (20 percent)				
0.6	60	541	1292	4852
	67	456	1033	4978
	80	461	978	5982
	80	536	1175	6450
	88	540	1147	7119
	95	462	903	7090
	100	460	886	7467
	100	417	786	7140
	105	459	881	7850
	105	408	748	7395
0.2	80	537	399	6450
	88	460	297	6572
	88	537	378	7104
	95	409	259	6803
	95	462	289	7085
	100	409	257	7035
	105	410	250	7380

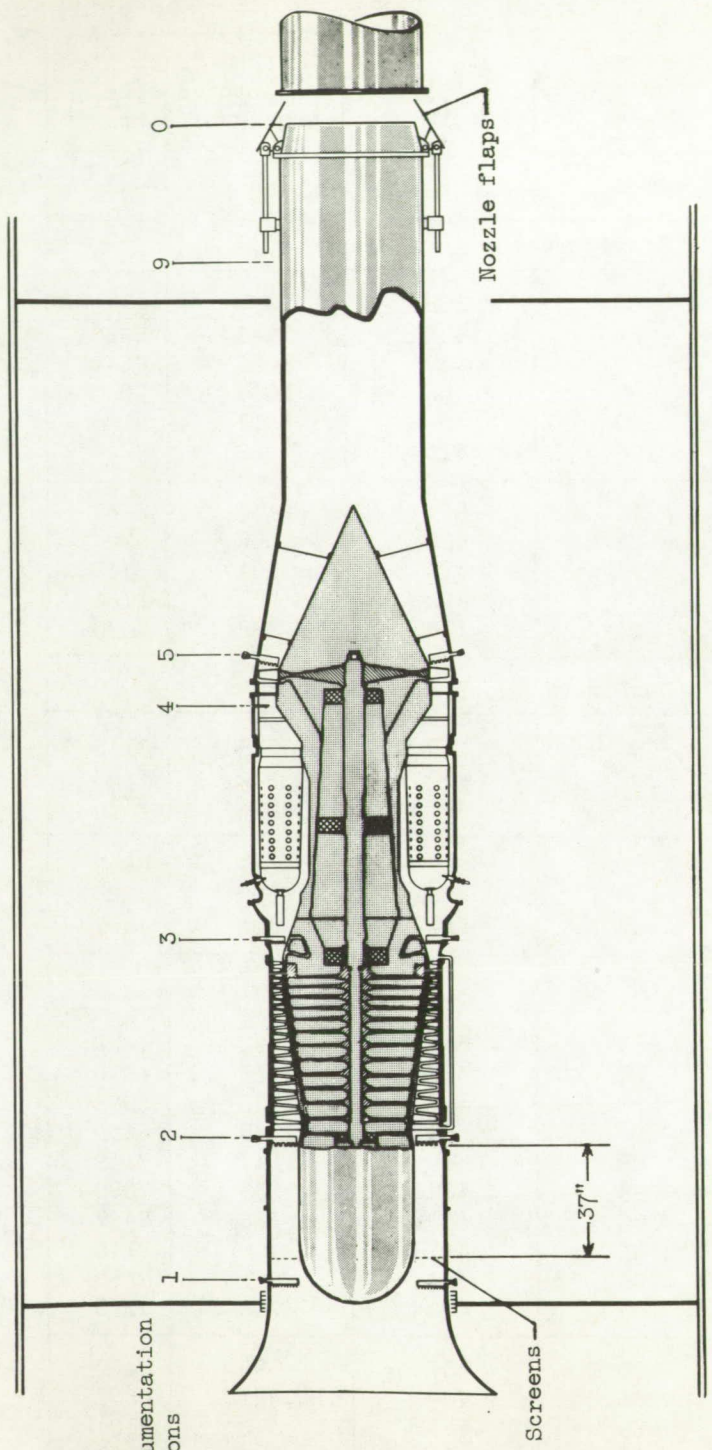

Figure 1. - Schematic diagram of engine installation in altitude test chamber showing location of instrumentation stations.

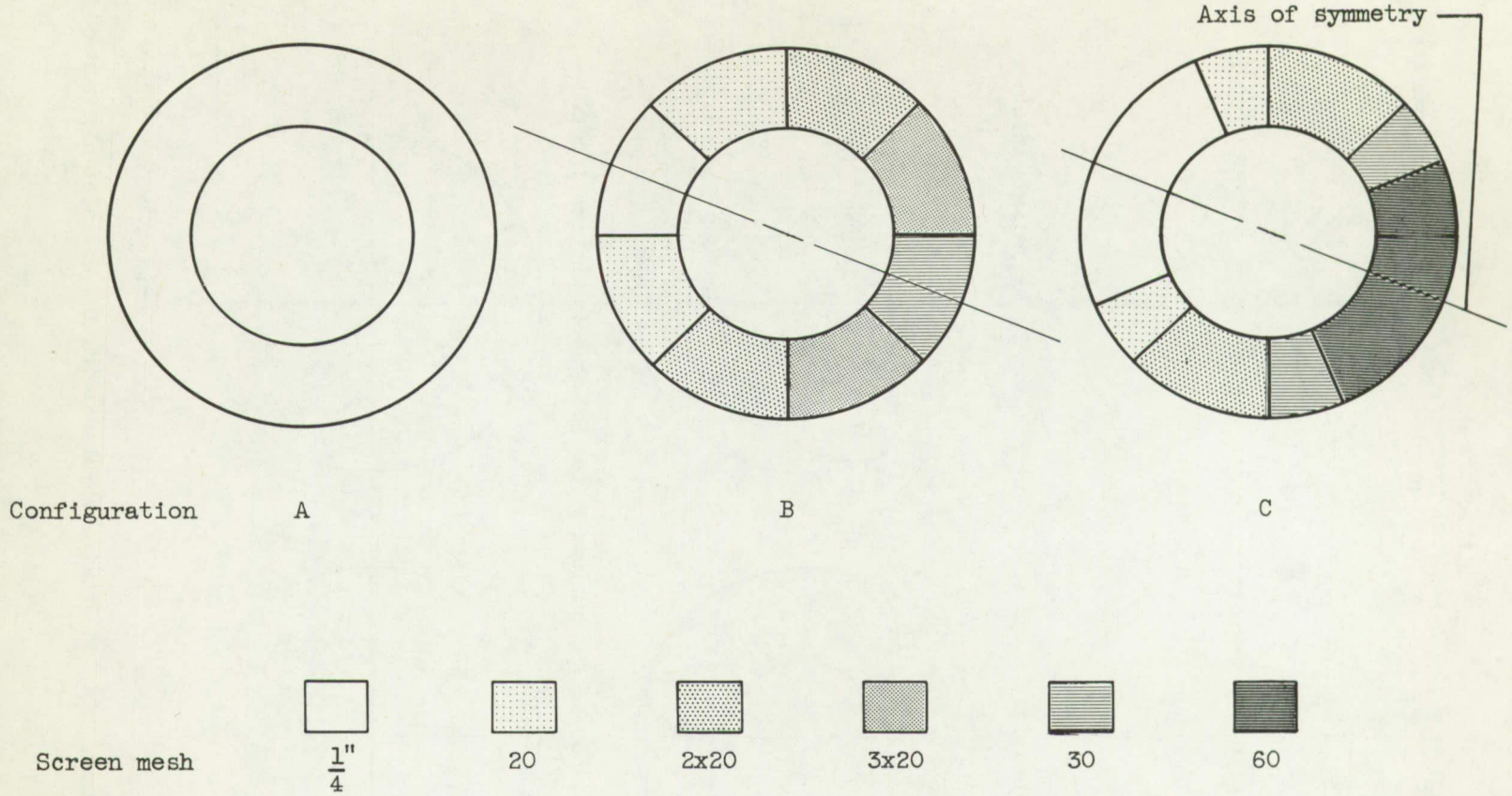

Figure 2. - Inlet-screen configurations.

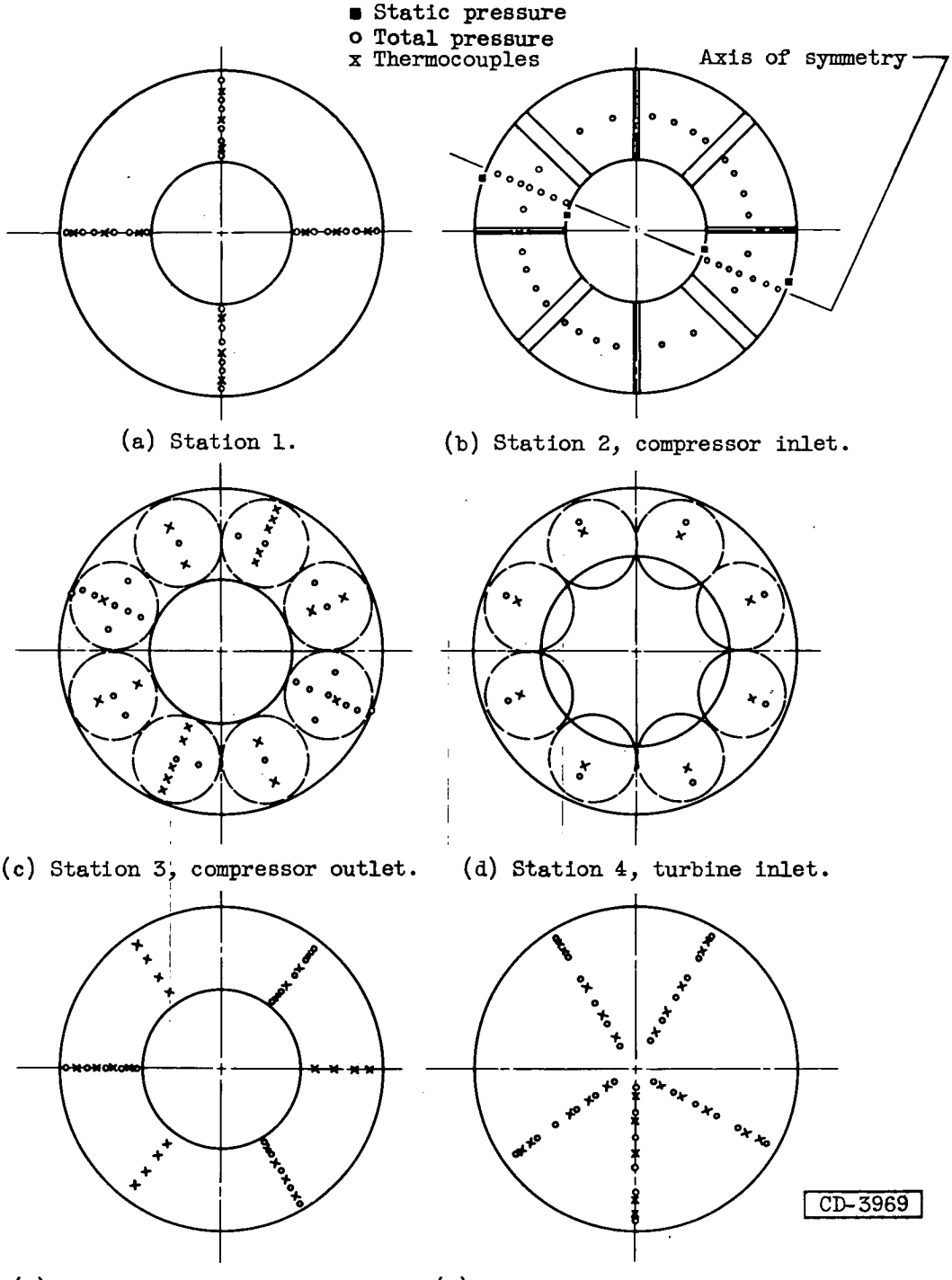

(a) Station 1. (b) Station 2, compressor inlet.

(c) Station 3, compressor outlet. (d) Station 4, turbine inlet.

(e) Station 5, turbine outlet. (f) Station 9, exhaust-nozzle inlet.

Figure 3. - Instrument station details for investigation of inlet-air distortion (looking downstream).

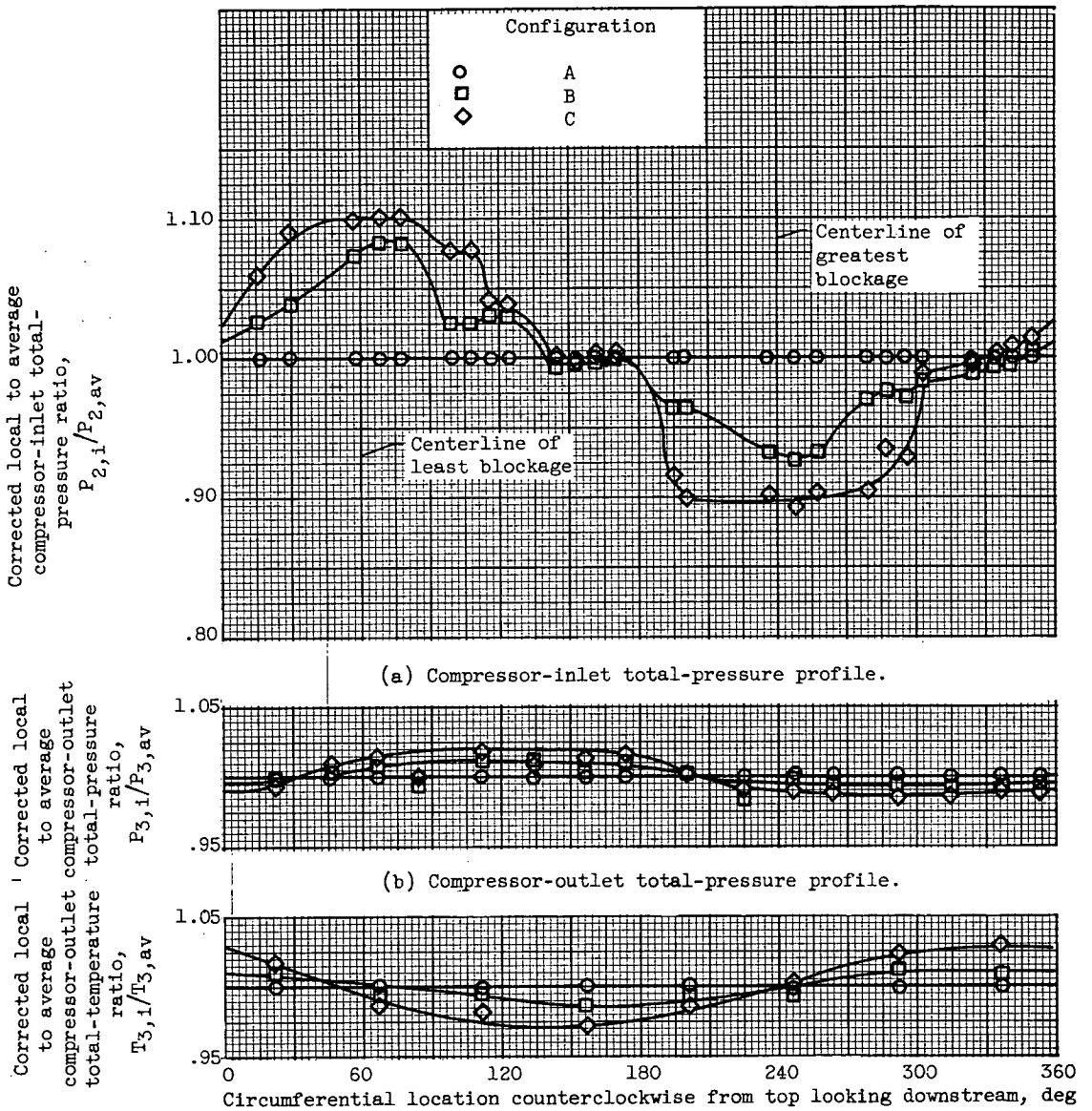

Figure 4. - Effect of inlet-air distortion on compressor pressure and temperature circumferential profiles. Corrected engine speed, 100 percent of rated; Reynolds number index, 0.6.

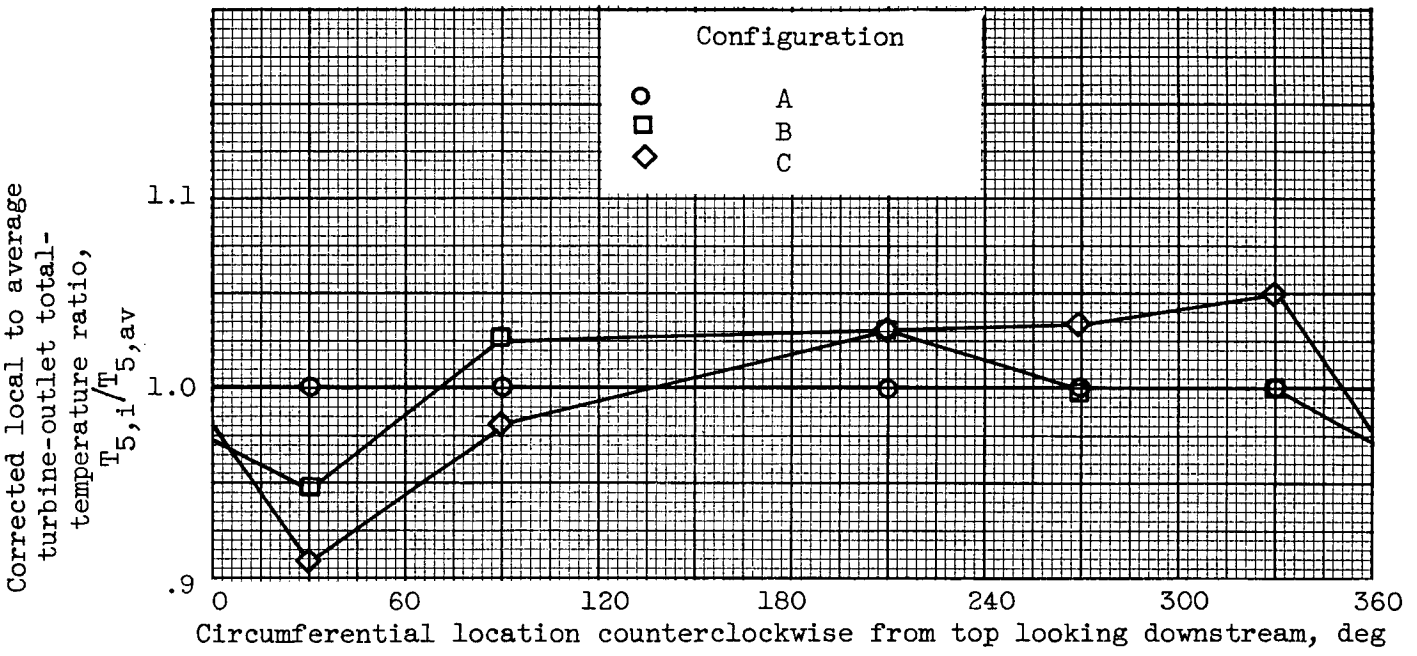

Figure 5. - Effect of inlet-air distortion on turbine-outlet total-temperature profile. Corrected engine speed, 100 percent of rated; Reynolds number index, 0.6.

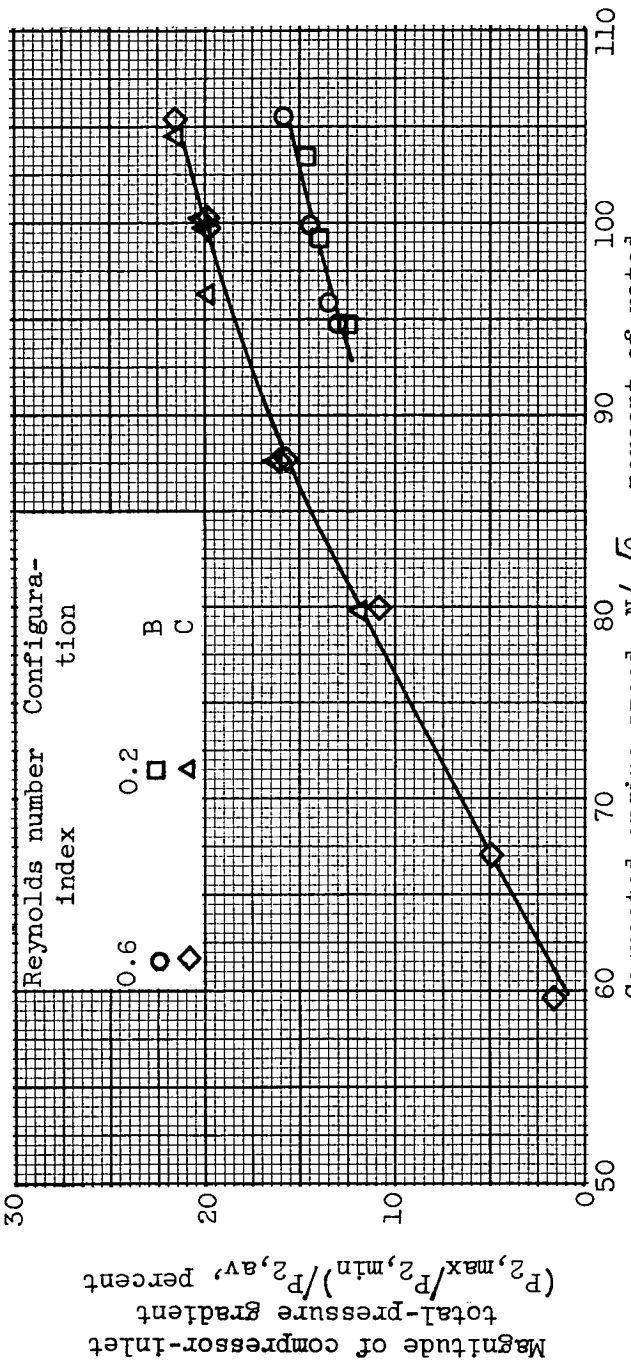

Figure 6. - Effect of corrected engine speed and Reynolds number index on magnitude of compressor-inlet total-pressure gradient.

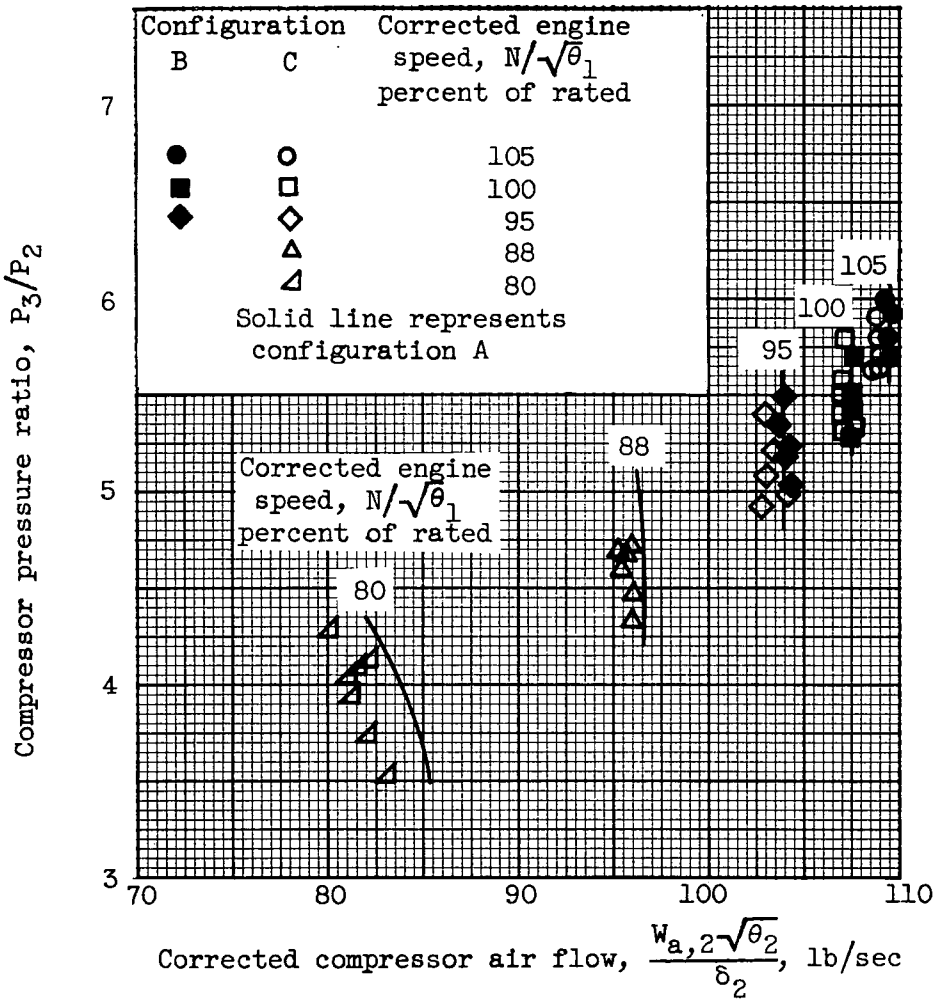

(a) Reynolds number index, 0.6.

Figure 7. - Effect of inlet-air distortion on over-all compressor map.

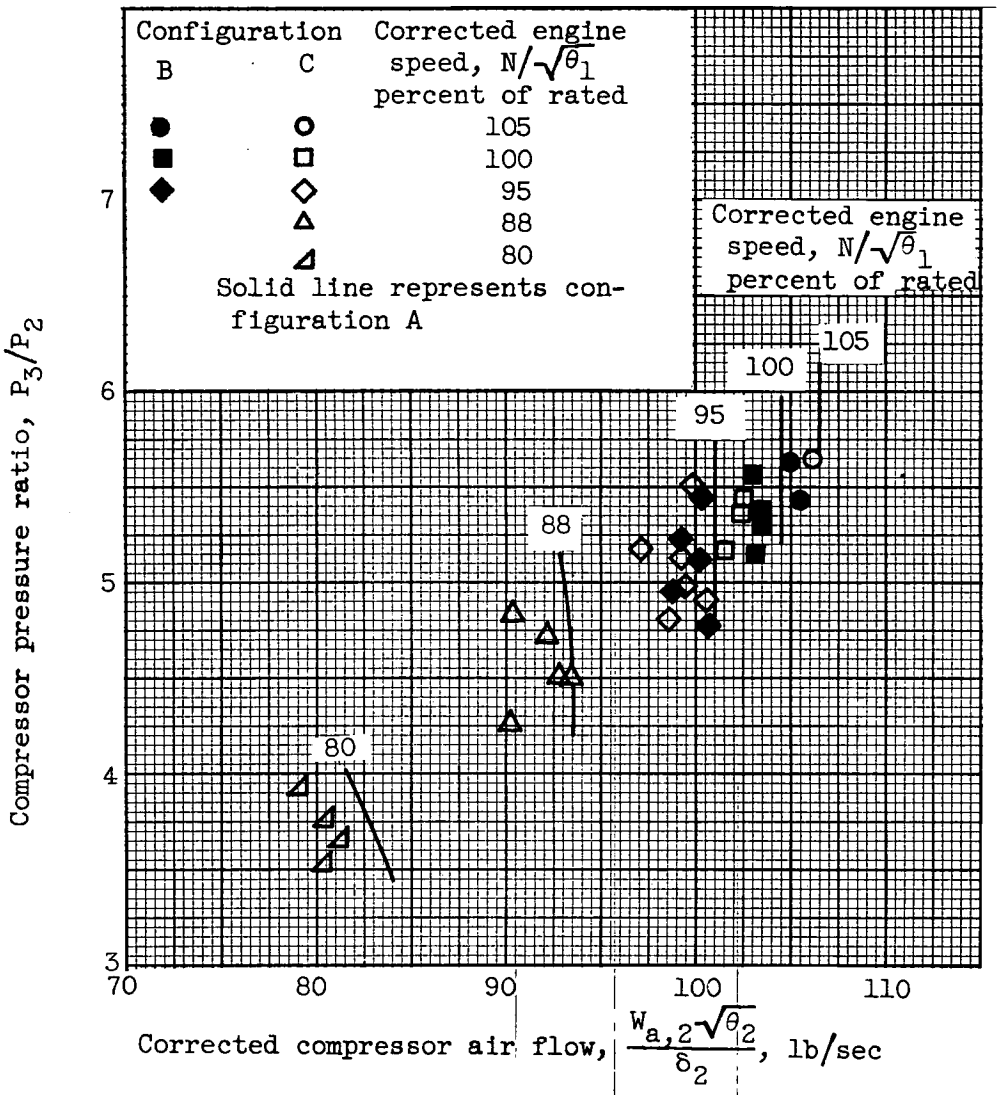

(b) Reynolds number index, 0.2.

Figure 7. - Concluded. Effect of inlet-air distortion on over-all compressor map.

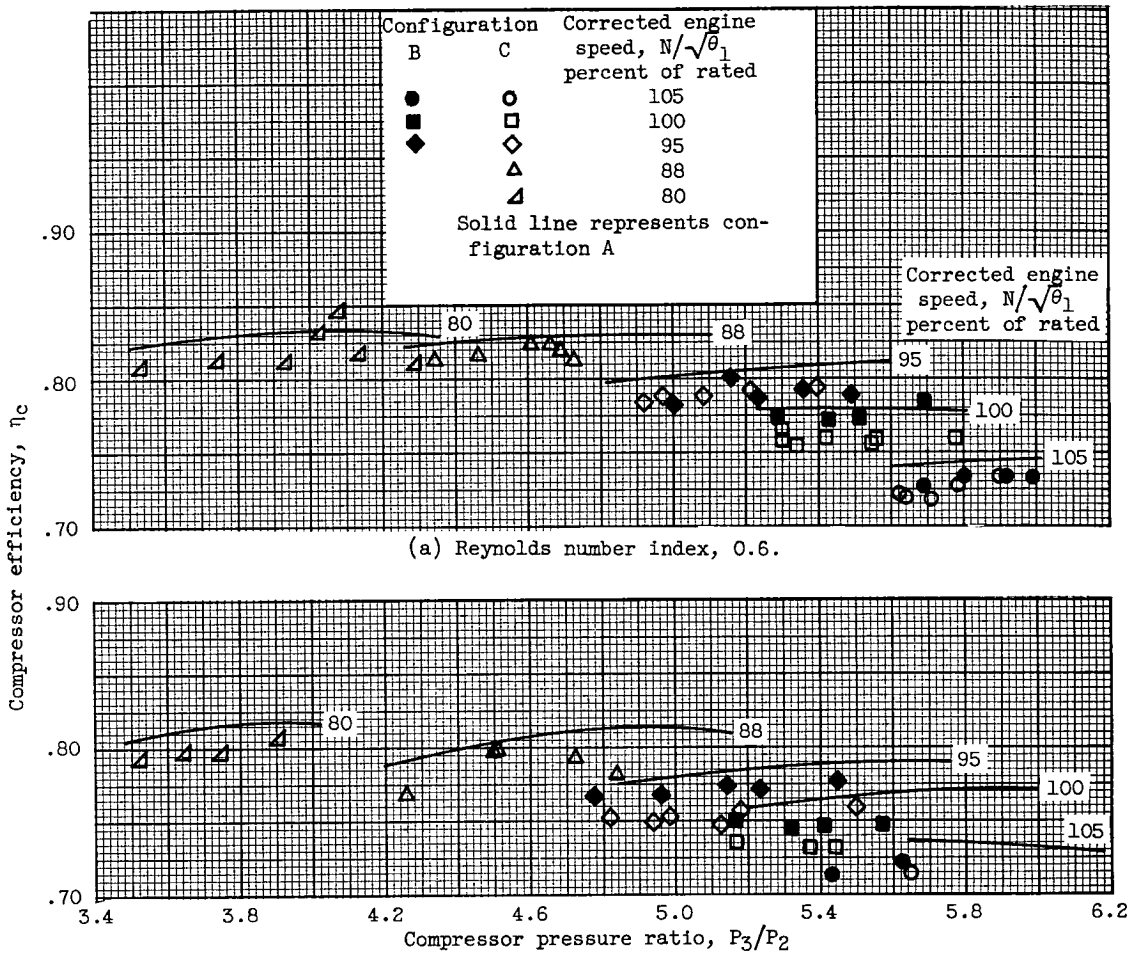

(a) Reynolds number index, 0.6.

(b) Reynolds number index, 0.2.

Figure 8. - Effect of inlet-air distortion on over-all compressor efficiency.

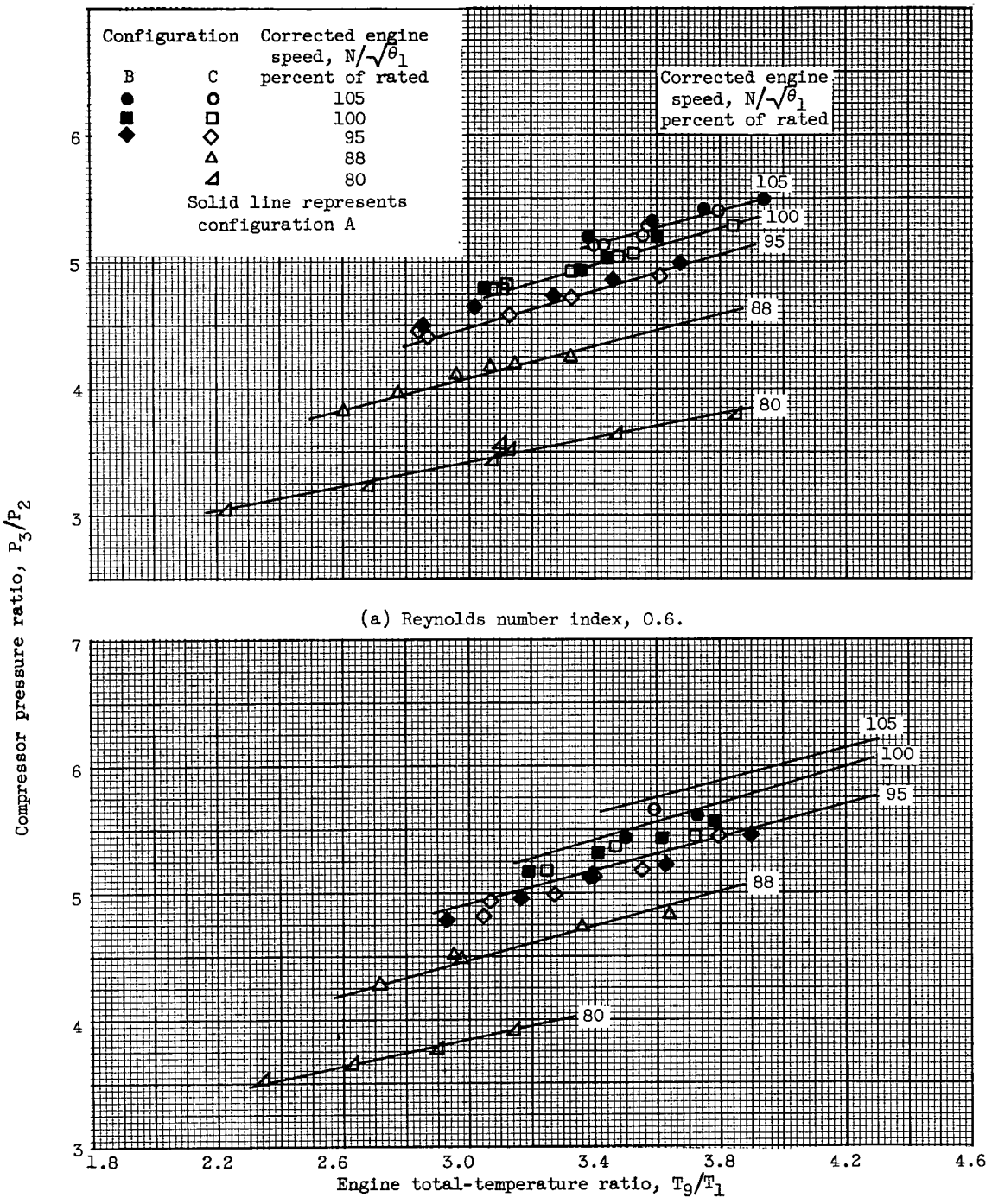

(a) Reynolds number index, 0.6.

(b) Reynolds number index, 0.2.

Figure 9. - Effect of inlet-air distortion on compressor pressure ratio as function of engine total-temperature ratio.

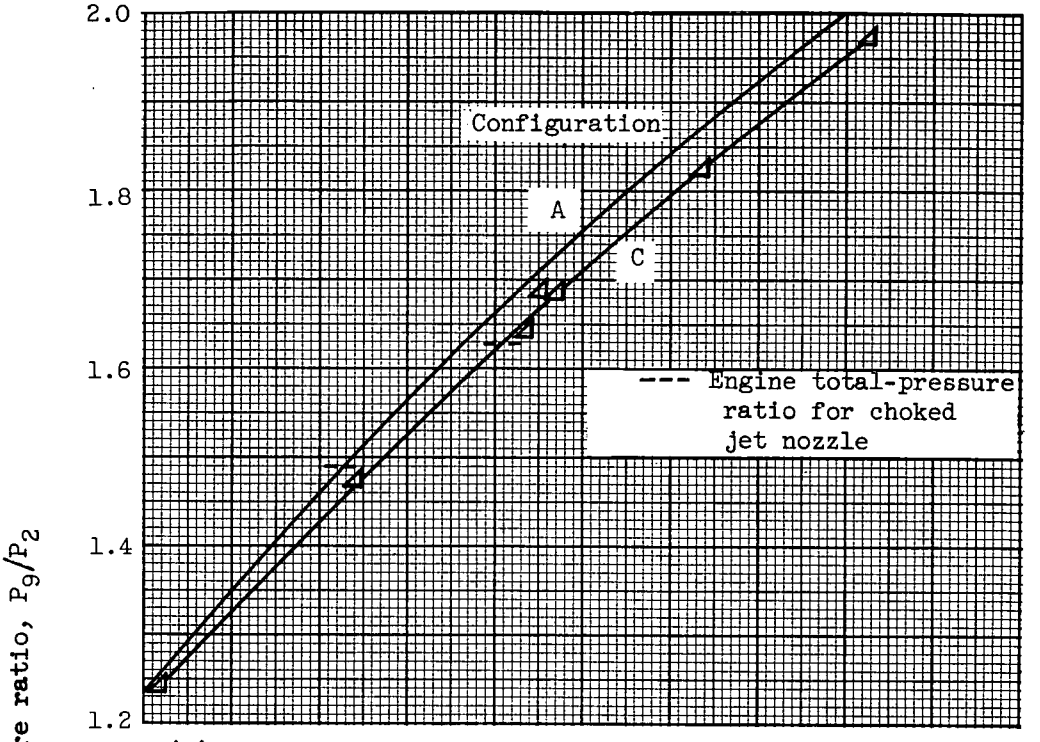

(a) Corrected engine speed, 80 percent of rated; Reynolds number index, 0.6.

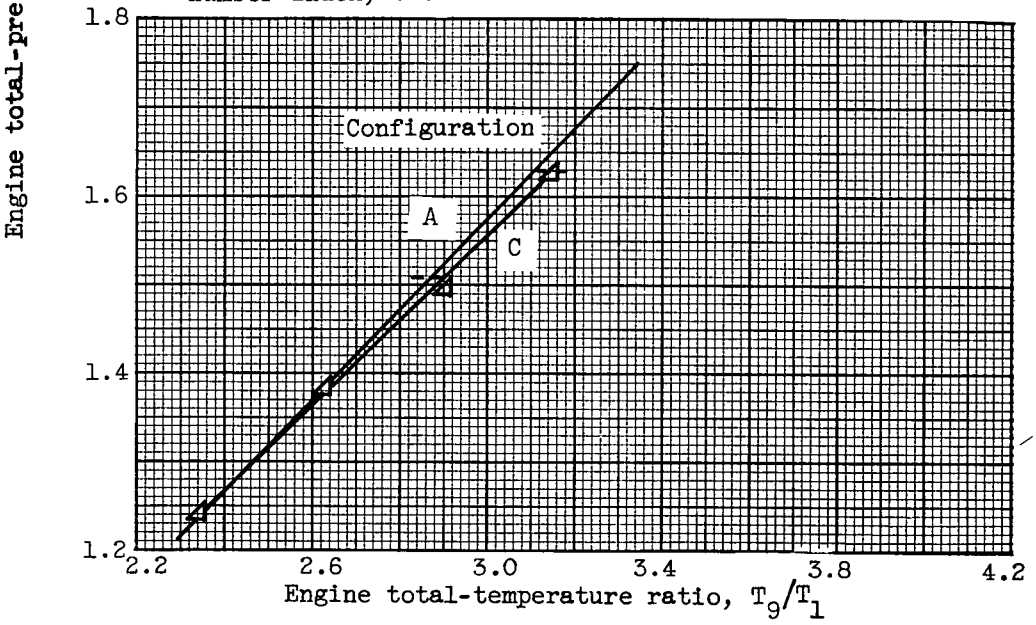

(b) Corrected engine speed, 80 percent of rated; Reynolds number index, 0.2.

Figure 10. - Effect of inlet-air distortion on engine pumping characteristics.

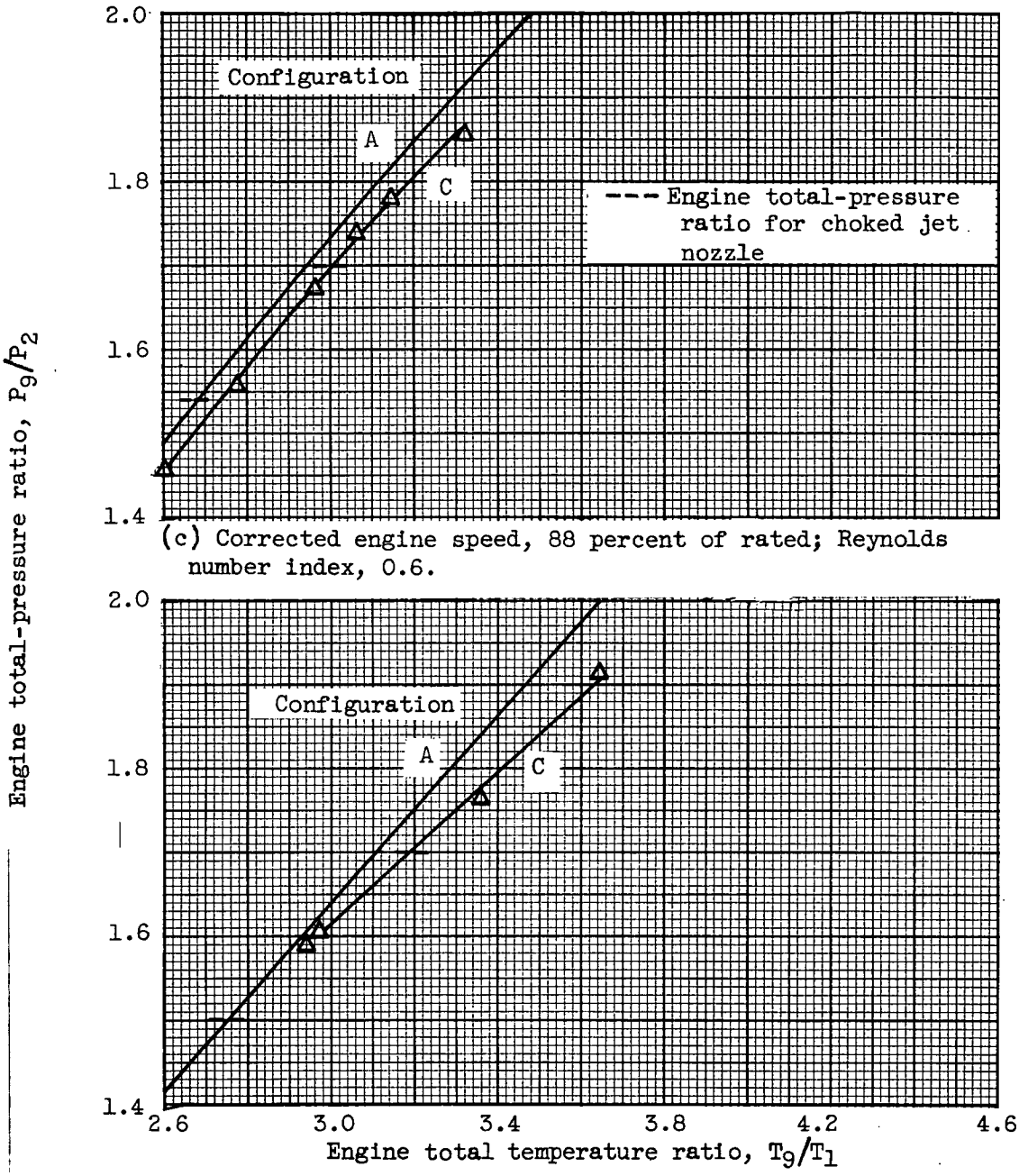

(c) Corrected engine speed, 88 percent of rated; Reynolds number index, 0.6.

(d) Corrected engine speed, 88 percent of rated; Reynolds number index, 0.2.

Figure 10. - Continued. Effect of inlet-air distortion on engine pumping characteristics.

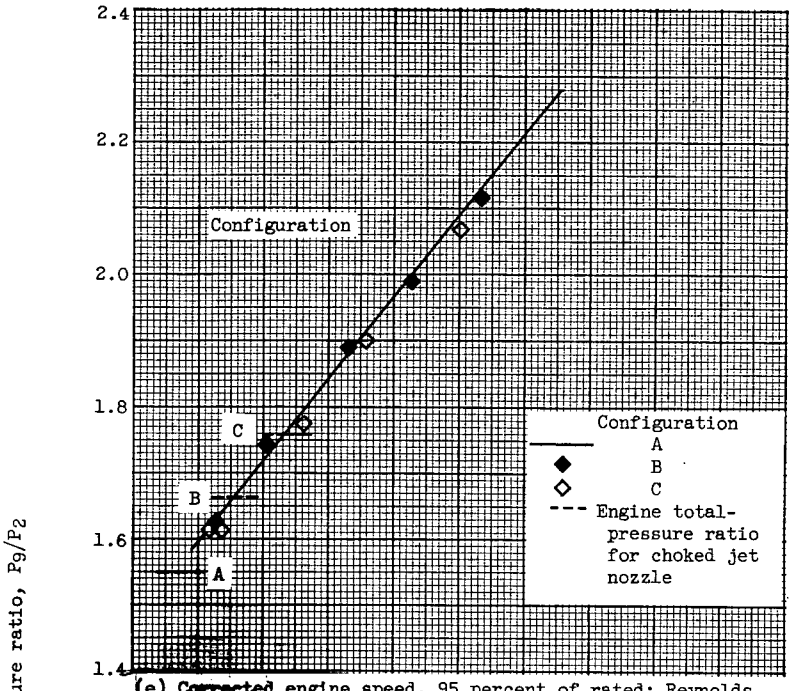

(e) Corrected engine speed, 95 percent of rated; Reynolds number index, 0.6.

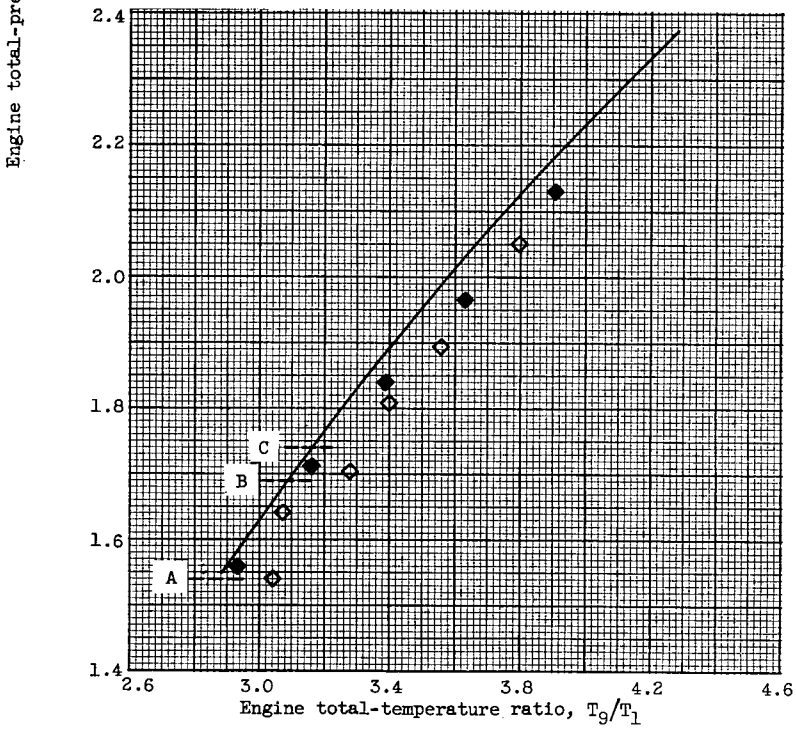

(f) Corrected engine speed, 95 percent of rated; Reynolds number index, 0.2.

Figure 10. - Continued. Effect of inlet-air distortion on engine pumping characteristics.

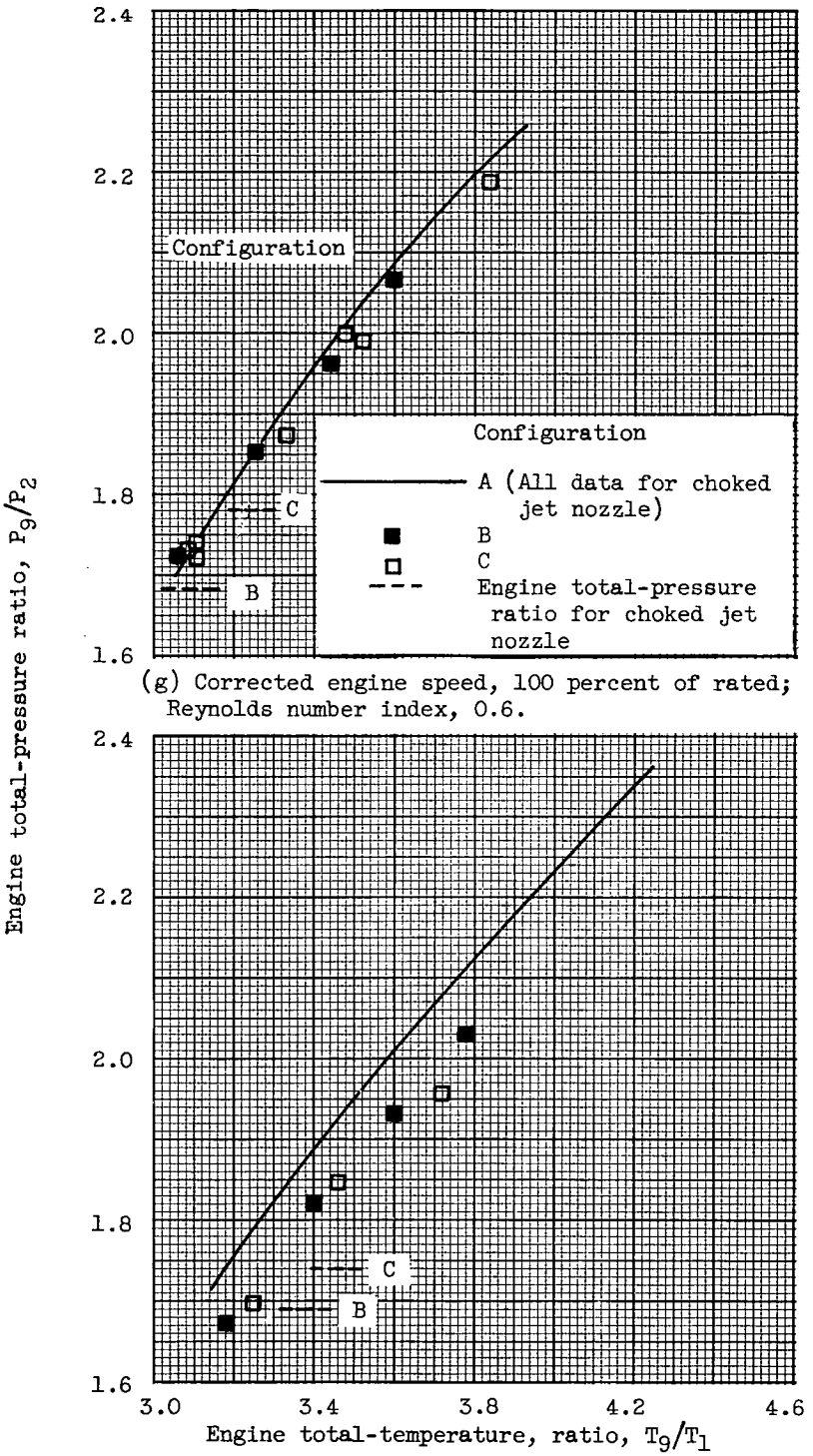

(g) Corrected engine speed, 100 percent of rated; Reynolds number index, 0.6.

(h) Corrected engine speed, 100 percent of rated; Reynolds number index, 0.2.

Figure 10. - Continued. Effect of inlet-air distortion on engine pumping characteristics.

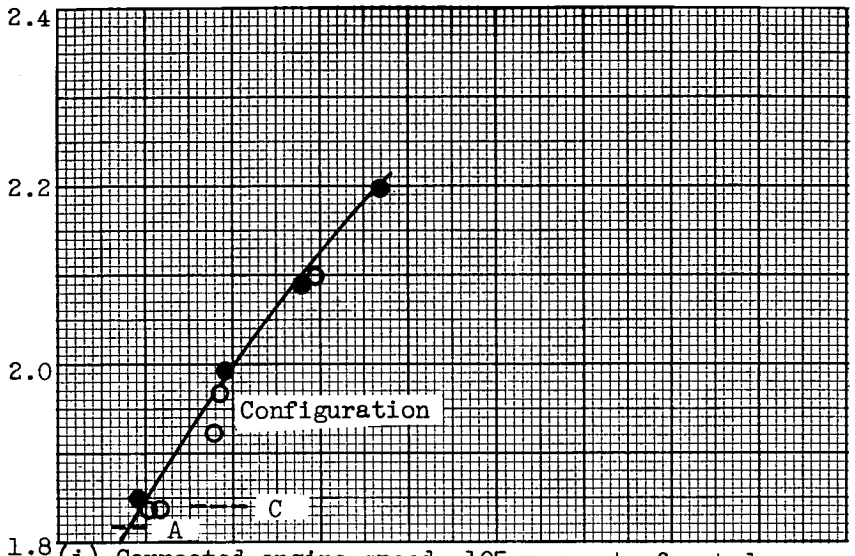

(i) Corrected engine speed, 105 percent of rated; Reynolds number index, 0.6.

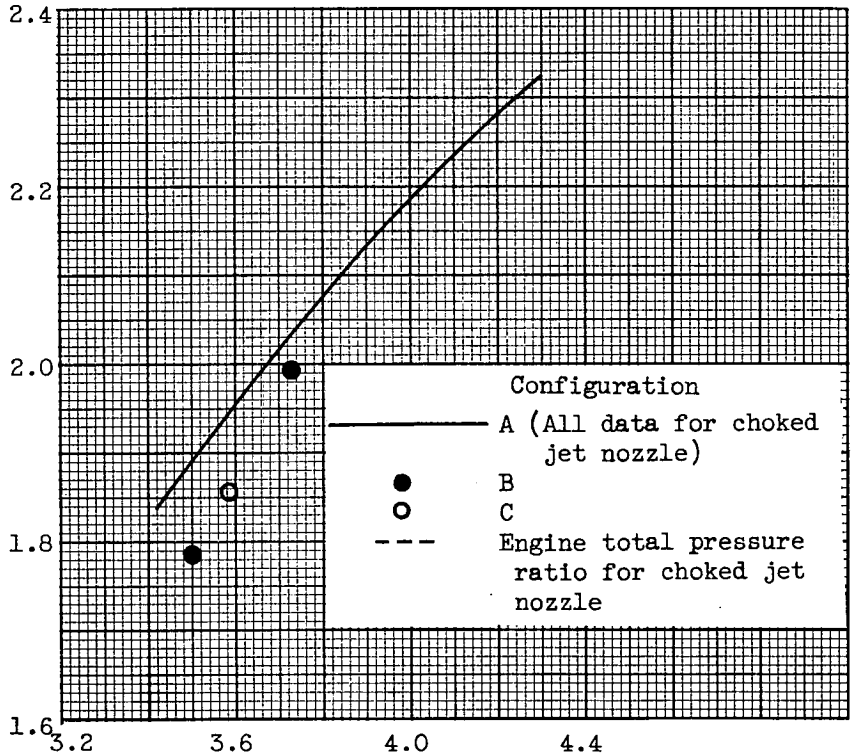

(j) Corrected engine speed, 105 percent of rated. Reynolds number index, 0.2. All data for choked jet nozzle.

Figure 10. - Concluded. Effect of inlet-air distortion on engine pumping characteristics.

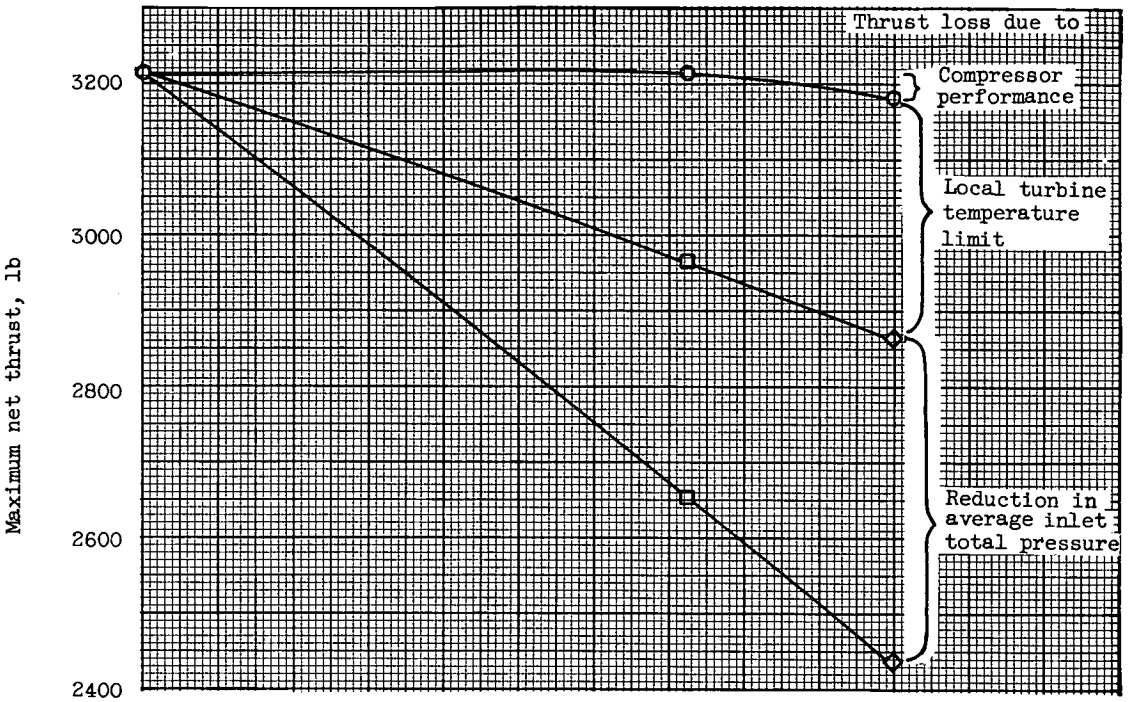

(a) Maximum net thrust.

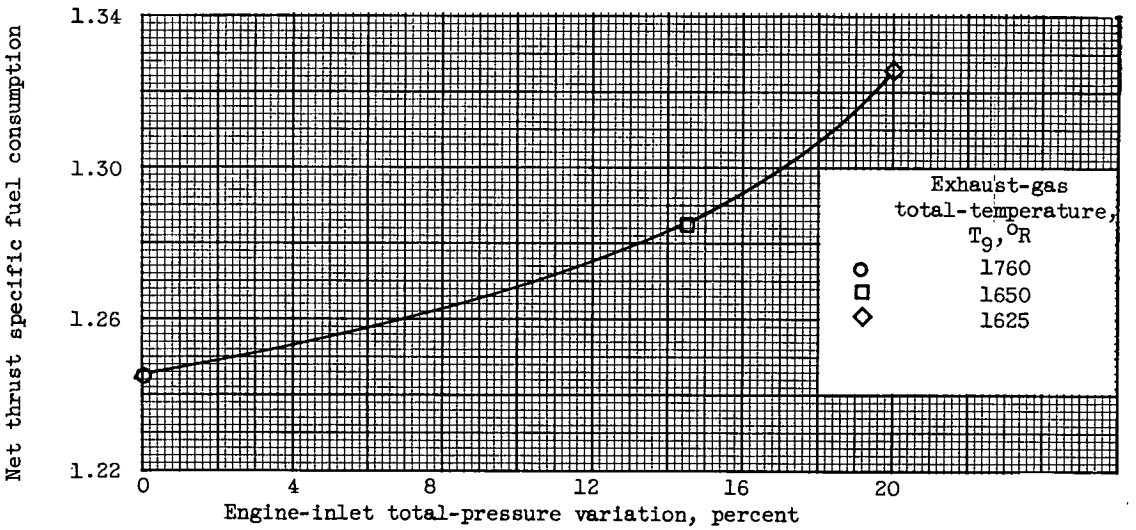

(b) Net thrust specific fuel consumption.

Figure 11. - Effect of inlet-air distortion on maximum net thrust and net thrust specific fuel consumption. Altitude, 22,000 feet; flight Mach number, 0.6; rated corrected engine speed.

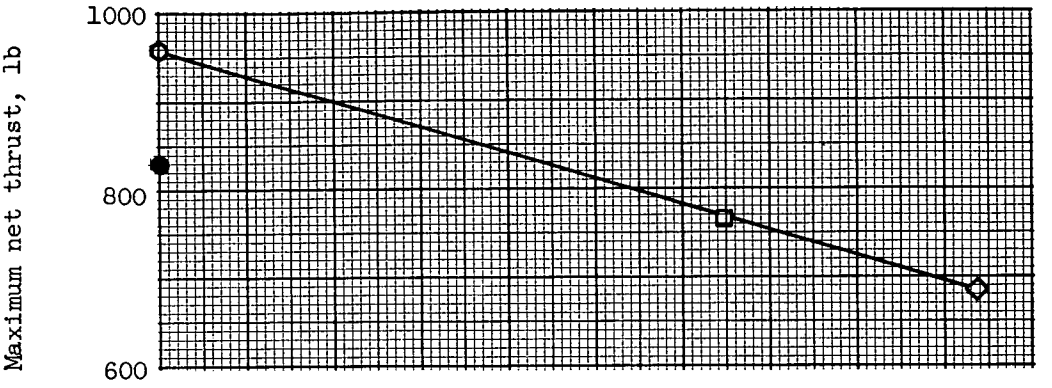

(a) Maximum net thrust.

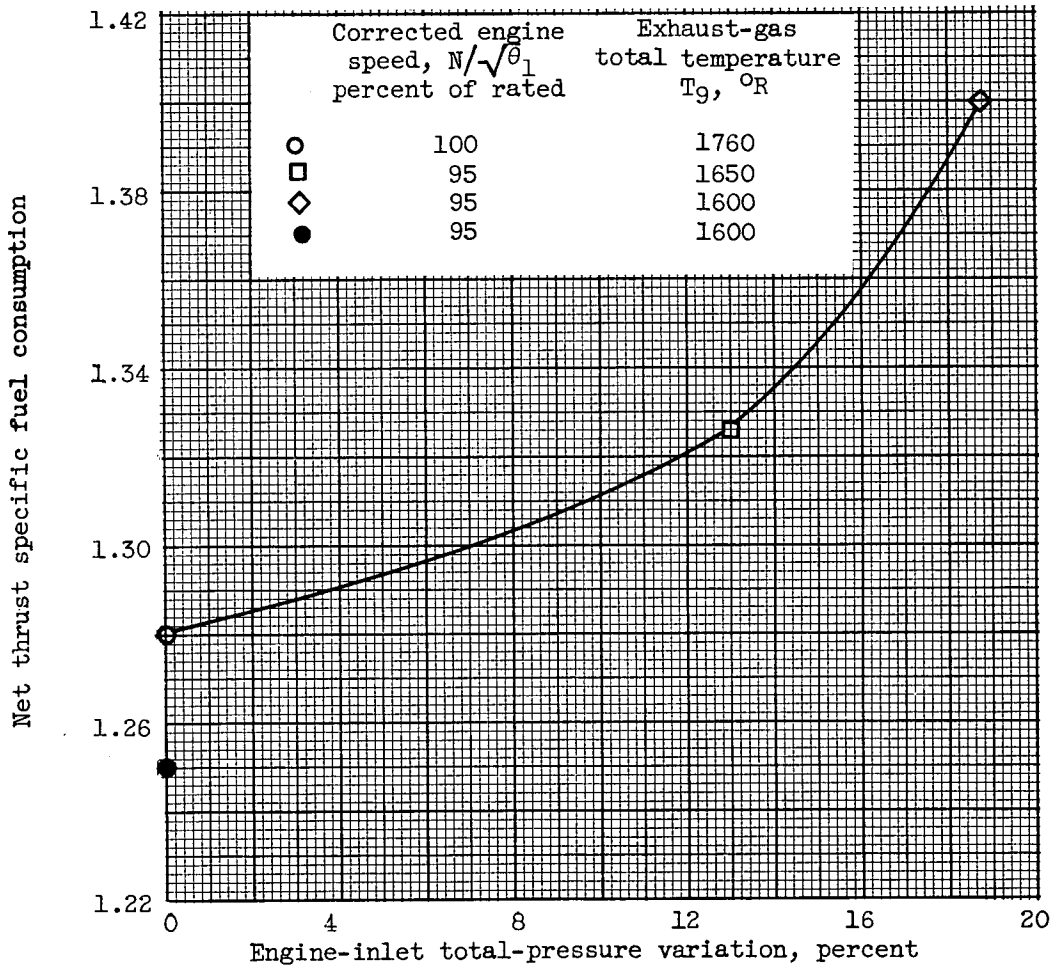

(b) Net thrust specific fuel consumption.

Figure 12. - Effect of inlet-air distortion on maximum net thrust and net thrust specific fuel consumption. Altitude, 50,000 feet; flight Mach number, 0.6; flight conditions based on maximum pressure at compressor inlet.

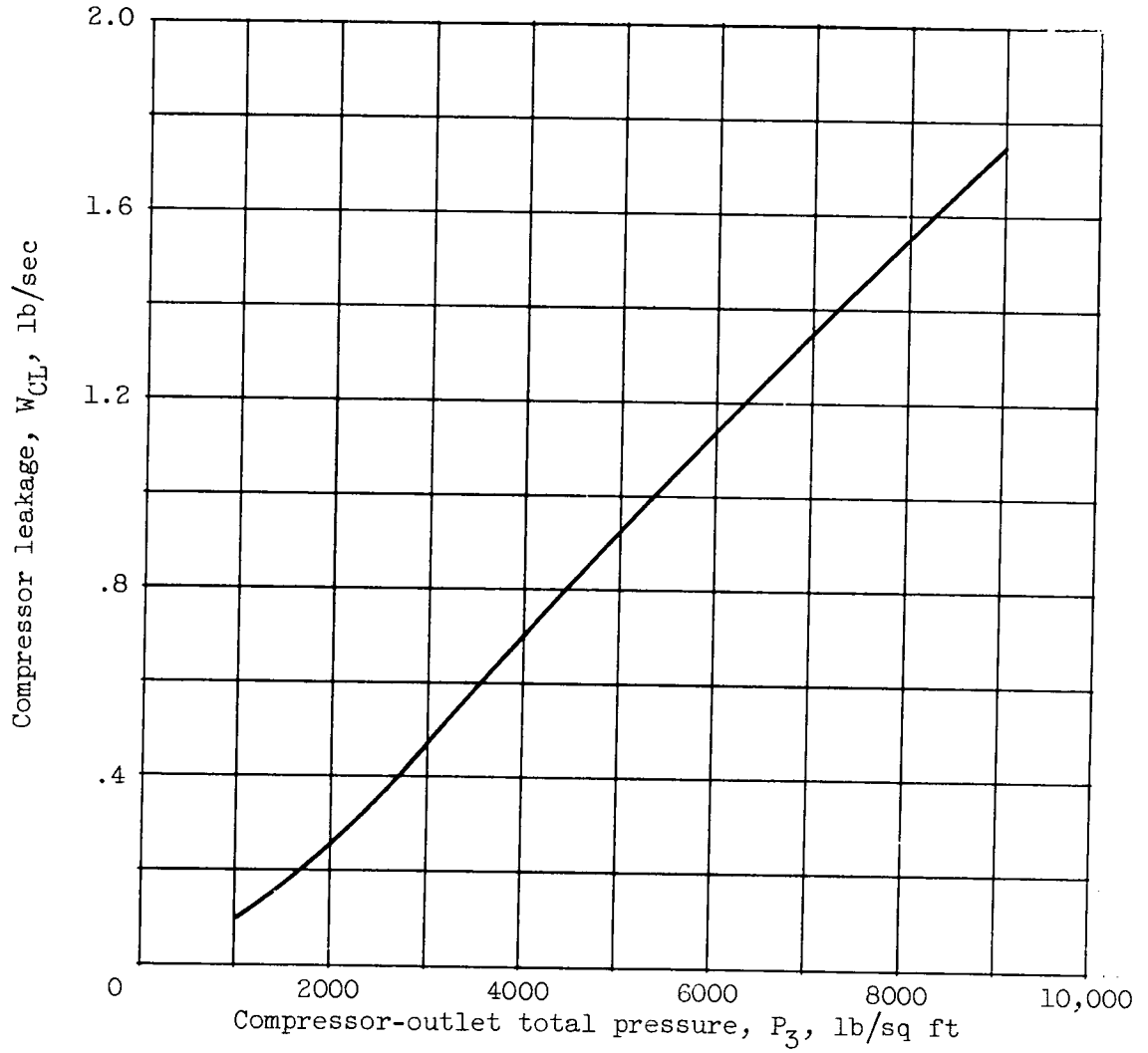

Figure 13. - Compressor leakage at engine midframe.

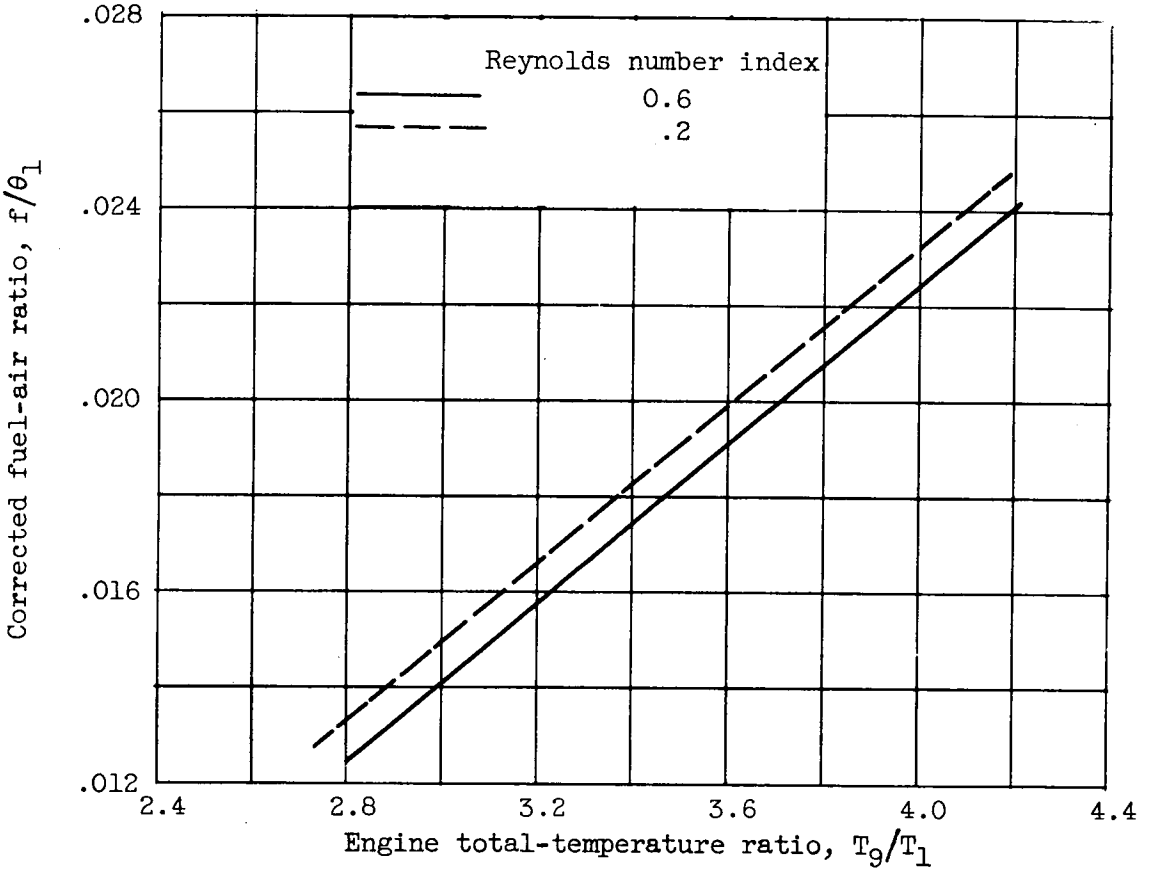

Figure 14. - Engine corrected fuel-air ratio.